



This is a repository copy of *Through-plane gas permeability of gas diffusion layers and microporous layer: Effects of carbon loading and sintering*.

White Rose Research Online URL for this paper:
<http://eprints.whiterose.ac.uk/113921/>

Version: Accepted Version

Article:

Orogbemi, O.M., Ingham, D.B., Ismail, M.S. et al. (3 more authors) (2017) Through-plane gas permeability of gas diffusion layers and microporous layer: Effects of carbon loading and sintering. *Journal of the Energy Institute*. ISSN 1743-9671

<https://doi.org/10.1016/j.joei.2016.11.008>

Article available under the terms of the CC-BY-NC-ND licence
(<https://creativecommons.org/licenses/by-nc-nd/4.0/>)

Reuse

Unless indicated otherwise, fulltext items are protected by copyright with all rights reserved. The copyright exception in section 29 of the Copyright, Designs and Patents Act 1988 allows the making of a single copy solely for the purpose of non-commercial research or private study within the limits of fair dealing. The publisher or other rights-holder may allow further reproduction and re-use of this version - refer to the White Rose Research Online record for this item. Where records identify the publisher as the copyright holder, users can verify any specific terms of use on the publisher's website.

Takedown

If you consider content in White Rose Research Online to be in breach of UK law, please notify us by emailing eprints@whiterose.ac.uk including the URL of the record and the reason for the withdrawal request.



eprints@whiterose.ac.uk
<https://eprints.whiterose.ac.uk/>

Title

Through-plane gas permeability of gas diffusion layers and microporous layer: effects of carbon loading and sintering

Authors

*O. M. Orogbemi, D.B. Ingham, M.S. Ismail, K. J. Hughes, L. Ma, M. Pourkashanian

Department of Mechanical Engineering, The University of Sheffield, S1 3JD, UK

* Corresponding author: Tel: +44 1142157220; fax: +44 113 246 7310

Email address: omorogbemi1@sheffield.ac.uk (O. M. Orogbemi)

Abstract

Knowledge of the absolute permeability for the various porous layers is necessary to obtain accurate profiles for water saturation within the membrane electrode assembly (MEA) in a two-phase model of a polymer electrolyte membrane fuel cell (PEMFC). In this paper, the gas permeability of gas diffusion layers (GDLs) coated with micro-porous layers (MPLs) of various carbon loadings for two different carbon blacks have been experimentally measured. The permeability of the GDL was found to decrease by at least one order of magnitude after the MPL-coating. Also, the permeability of the MPLs was shown to be lower than that of the carbon substrate by 2-3 orders of magnitude. Further, it was found that the gas permeability of the MPLs changes significantly from one carbon loading to another despite the use of a single weight composition for all the MPLs coated, namely 20% PTFE and 80% carbon black. This signifies the possible inaccuracy in estimating the MPL permeability through employing the cross-section SEM images as they do not resolve the MPL penetration into the carbon substrate. Finally, the MPL sintering was found to slightly decrease the permeability of the GDL.

Keywords: PEMFCs; GDL; MPL; Carbon loading; Carbon type, Sintering; Gas permeability

1. Introduction

Polymer electrolyte membrane fuel cells (PEMFCs) are a promising clean power source for a wide range of portable, automotive and stationary applications and this is in particular due to its high efficiency and low-temperature start-up [1-6]. Gas diffusion layers (GDLs) are key components in PEMFCs [7-10]. The GDL is a porous layer sandwiched between the catalyst layer (CL) and the flow-field plate. The main functions of the GDL are to uniformly and efficiently distribute the reactant gases to the catalyst layer; improve the electrical contact with the latter; dissipate heat that is mainly generated in the cathode catalyst layer; and drive excessive liquid water away from the electrodes to the flow channels [11-18]. To efficiently perform the above functions, the GDL is usually wet-proofed [19-24]. Further, it is normally coated with the so-called micro-porous layer (MPL) on the side facing the catalyst layer in order to enhance the electrical contact with the catalyst layer and properly handle the liquid water emerging from the cathode catalyst layer. The MPL is typically composed of carbon black and PTFE particles [21].

Many researchers have investigated the effects of the MPL and its composition on the performance of PEMFCs [7, 9, 25-31]. The areas of research in this regard are typically on the effects of loading of the wet-proofing agent [25, 27-28, 31, 45], type of carbon black [6, 22, 26, 32] and carbon loading [21, 25, 27-28, 45]. Park et al. [26] found that the optimum carbon loading that achieves the maximum performance is 0.5 mg cm^{-2} . Ismail et al. [25] measured the through-plane permeability of two coated GDLs that varied in terms of PTFE loading present in the MPL. They found that the through-plane permeability of the MPL, and consequently the permeability of the whole GDL, increases as the PTFE loading increases from about 25% to 50%. Jordan et al. [22] reported that a better fuel cell performance is achieved

when the loading of the Acetylene Black carbon is between about 1.25 and 1.9 mg cm⁻². In addition, they investigated the influence of carbon black types, i.e., Vulcan XC-72R and Acetylene Black, and sintering on the fuel cell performance. They found that the cell performs better with the sintered MPL loaded with Acetylene Black carbon and this is mainly due to the uniform distribution of the PTFE loading in the sintered MPL. It is worth mentioning that sintering is performed to coalesce the PTFE particles by subjecting them to a temperature close to their melting point and consequently uniformly distribute them in the MPL [8]. Similarly, the PTFE loading in the carbon substrate has an influence on the overall performance of the PEMFCs [23, 25, 27-28].

For two-phase modelling of PEMFCs, it is of importance to use accurate values for the permeability of the various porous layers in the membrane electrode assembly (MEA). The permeability significantly affects the capillary diffusivity and consequently the saturation profile within the MEA [19, 32]. The gas permeability of the GDL has been experimentally estimated by various research groups [33-45]. However, there have been fewer attempts to estimate the permeability of thinner layers, namely the MPL and the catalyst layers [21, 25, 33-34]. In this paper, we have experimentally estimated the permeability of the MPLs of in-house coated GDLs through measuring the permeability and thickness values of the GDL before and after MPL-coating. The sensitivity of the MPL permeability to carbon loading of the MPL with different carbon types has been investigated for the first time. Further, we shed some light on the effects of sintering on the permeability of the coated GDLs.

2. Materials and Methods

The carbon substrate used to prepare the coated GDLs was SGL 10BA which was provided by SGL Carbon GmbH, Meitingen, Germany. The physical properties of the SGL 10BA carbon substrate, as provided by the manufacturer, are listed in Table 1. Two types of carbon powders were considered, Ketjenblack EC-300J (AkzoNobel, the Netherlands) and Vulcan XC-72R (Cabot Corporation, USA). Table 2 summarises the physical properties of the carbon blacks as provided by the manufacturers. The hydrophobic agent used was 60 wt% PTFE emulsion (Sigma-Aldrich, UK).

Table 1: Manufacturer’s physical properties of the SGL 10BA carbon paper substrate.

Physical parameter	Reported value
Thickness	$380 \pm 60 \mu\text{m}$
Areal weight	$85 \pm 2 \text{ g m}^{-2}$
Porosity	0.88
PTFE loading	5 % by weight

Table 2: Manufacturer's physical properties of the carbon black.

Properties	Ketjenblack EC-300J	Vulcan XC-72R
Pore volume (ml/100 g)	310-345	178
Apparent bulk density (kg/m ³)	125-145	20-380
Surface area (m ² /g)	950	254
Particle diameter (nm)	30	30
pH	9.0-10.5	2-11
Volatile (by weight % max.)	1.0	2-8

2.1 Preparation and application of MPL ink

For the purpose of this study, 5 sets of MPL-coated GDL samples were prepared following the procedures available in [22, 26]. In each set, there were 6 samples which share the same carbon loading in the MPLs. The carbon loadings considered were 0.5, 1.0, 1.5, 2.0 and 2.5 mg cm⁻². The difference between the each set of the 6 samples illustrated below in Fig. 5, Section 3.2. For all the carbon loadings investigated, the composition by weight of the MPL ink has been kept unchanged: 80 % carbon powder and 20 % PTFE. The calculated amounts of the carbon black and the PTFE dispersion were manually mixed until a paste-like material was formed. Isopropyl alcohol was added, as a dispersion agent to the formed mixture and the resulting slurry was sonicated until an ink with a good dispersion was formed. The carbon substrate samples were stuck to a heated plate and the formed ink was manually sprayed onto them using a spray gun (Badger 100TM LG, USA). In this work, nitrogen gas is used for applying the ink slurry on the surfaces of the samples [26]. The temperature of the plate was set to about 80 °C

in order to evaporate the volatile components as the ink was applied to the substrate. The samples of the carbon substrates were made circular with a 2.50 cm diameter [39].

The thickness of the GDL samples was measured before and after the MPL-coating using a micrometre. Each sample was measured at 4 equally-spaced positions within it to provide a representative average value of the thickness. The thickness of the coated samples was confirmed by employing cross-section scanning electron microscopy (SEM) images. These images were also used in estimating the thickness of the MPL which was required in calculating its gas permeability, as will be shown in Section 2.4. The SEM images were produced using MA15SEM (EVOZEISS, 80 mm²).

2.2 Sintering

The MPL-coated GDL samples were heat-treated as follows: 120 °C for 1 hour, 280 °C for 30 minutes and finally sintered at a temperature of 350 °C for 30 minutes. It should be noted that the gas permeability of the coated samples were experimentally measured before and after heat-treatment and sintering in order to evaluate the effects of the latter process. The morphology of the MPLs before and after heat-treatment was examined by employing SEM images of the surfaces of the coated samples.

2.3 Through-plane gas permeability setup

The experimental setup of this work has been previously used in [27] for investigating through-plane permeability, see Fig. 1. As shown in Fig. 1, the setup consists of upper and lower fixtures, with the sample fixed between the two fixtures as described in [22]. Nitrogen gas was the flowing gas through the sample. The pressure drop across the sample was measured at 8 equal-interval values of the flow rate. The flow controller used was an HFC-202 (Teledyne

Hastings, UK) with a range of 0.0 – 0.5 SLPM and the differential pressure sensor used was a PX653 (Omega, UK) with a range of ± 12.5 Pa.

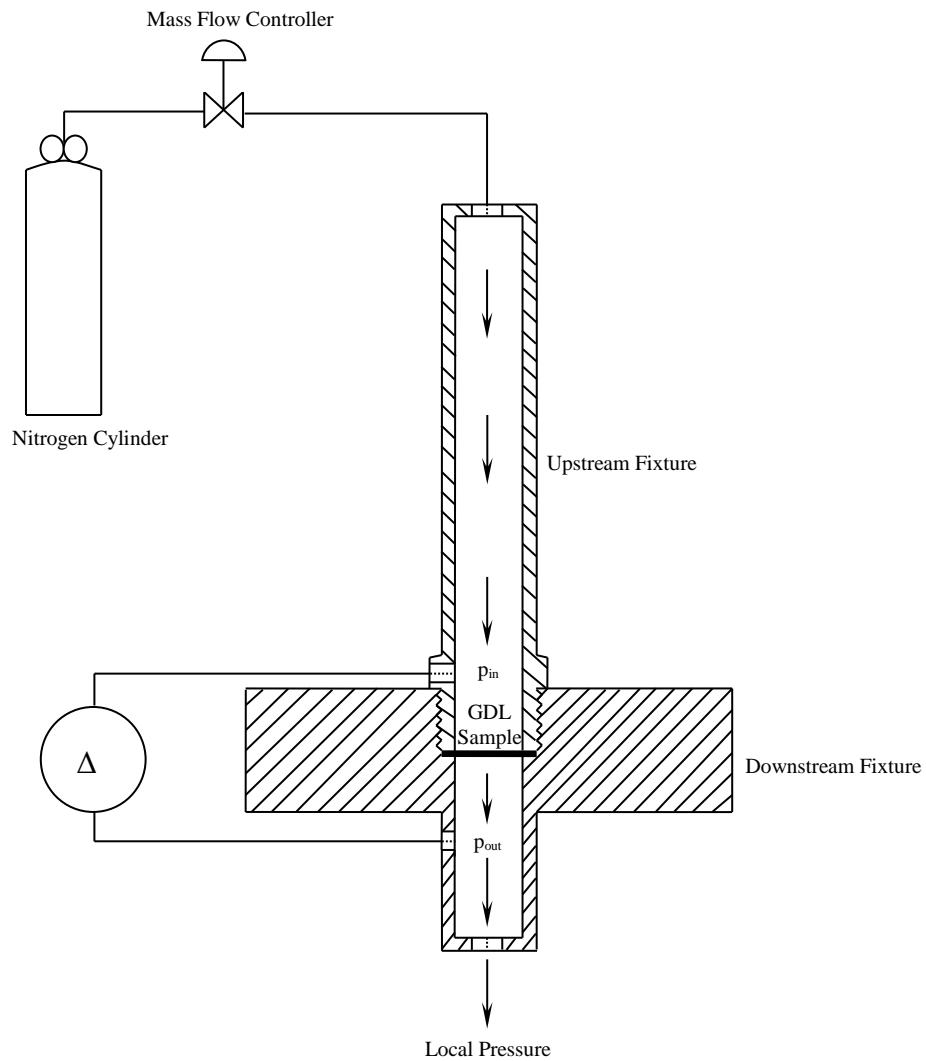


Fig. 1: Schematic diagram of the experimental setup. Reprinted from Ref. [26] with permission of Elsevier.

2.4 Data analysis

Sufficiently low flow rates were used to render the inertial losses negligible and consequently Darcy's Law is employed, which can be solved for the permeability as follows [31]:

$$\frac{\Delta P}{L} = \frac{\mu}{k} v \quad (1)$$

$$v = \frac{Q}{\pi D^2} \quad (2)$$

where ΔP is the pressure drop across the sample, L is the thickness of the sample, μ is the dynamic viscosity of nitrogen gas, k is the gas permeability of the porous sample calculated at the test temperature (~ 20 °C), v is the velocity of the flowing gas, Q is the volumetric flow rate and D is the diameter of the sample exposed to the flow.

Since the carbon substrate and MPL are typically layered in the coated GDLs, the pressure drop across the coated sample can be consequently expressed as follows [42]:

$$\Delta P_{\text{GDL}} = \Delta P_{\text{MPL}} + \Delta P_{\text{sub}} \quad (3)$$

where ΔP_{GDL} , ΔP_{MPL} and ΔP_{sub} are the pressure drops across the coated GDL, the MPL and the carbon substrate, respectively. From Equation (1), Equation (3) can be written as follows:

$$\frac{\mu L_{\text{GDL}}}{k_{\text{GDL}}} v = \frac{\mu L_{\text{MPL}}}{k_{\text{MPL}}} v + \frac{\mu L_{\text{sub}}}{k_{\text{sub}}} v \quad (4)$$

where L_{GDL} , L_{MPL} and L_{sub} are the thicknesses of the coated GDL, the MPL and the carbon substrate respectively, and k_{GDL} , k_{MPL} and k_{sub} are the gas permeability coefficients for the coated GDL, the MPL and the carbon substrate, respectively. Clearly one can make use of Equation (4) to solve for the permeability of the MPL [25]:

$$k_{\text{MPL}} = \frac{L_{\text{MPL}}}{\frac{L_{\text{GDL}}}{k_{\text{GDL}}} - \frac{L_{\text{sub}}}{k_{\text{sub}}}} \quad (5)$$

As mentioned in Section 2.1, the thickness of the MPL was estimated locally using cross-section SEM images at as many points as possible in order to have a well-representative value of the thickness of the MPL, see Figure 8.

3. Results and Discussion

3.1 Through-plane permeability of the carbon substrate

The gas permeability of the carbon substrate used was estimated by fitting the experimental data of the pressure gradients as a function of the velocity to Eq. (1). Figure 2 shows a typical pressure gradient-velocity experimental data used to calculate the gas permeability of carbon substrate.

The average thickness of 30 carbon paper substrate samples was estimated to be about $370 \pm 40 \mu\text{m}$. The averaged through-plane gas permeability for the carbon substrate samples was found to be $1.77 \times 10^{-11} \text{ m}^2$. This value is in good agreement with those reported in the literature for the same substrate, namely Ihonen et al. ($1.80 \times 10^{-11} \text{ m}^2$) [23], Gostick et al. ($3.74 \times 10^{-11} \text{ m}^2$) [33] and Ismail et al. ($2.72 \times 10^{-11} \text{ m}^2$) [25].

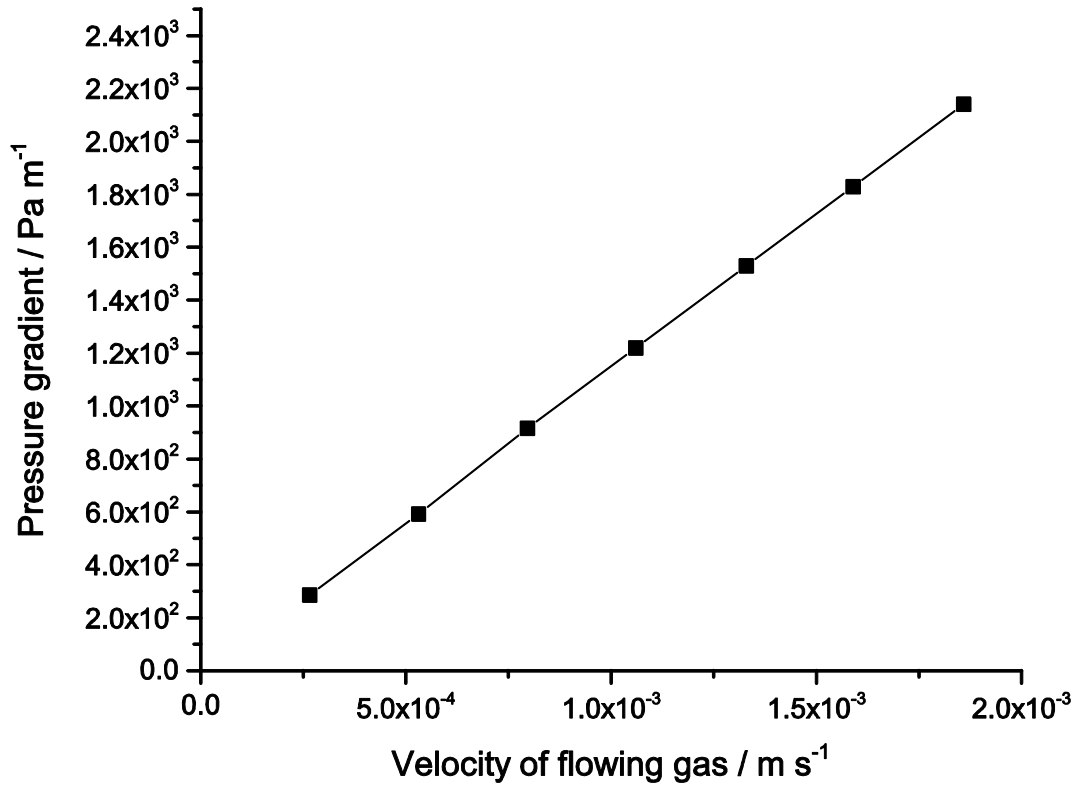


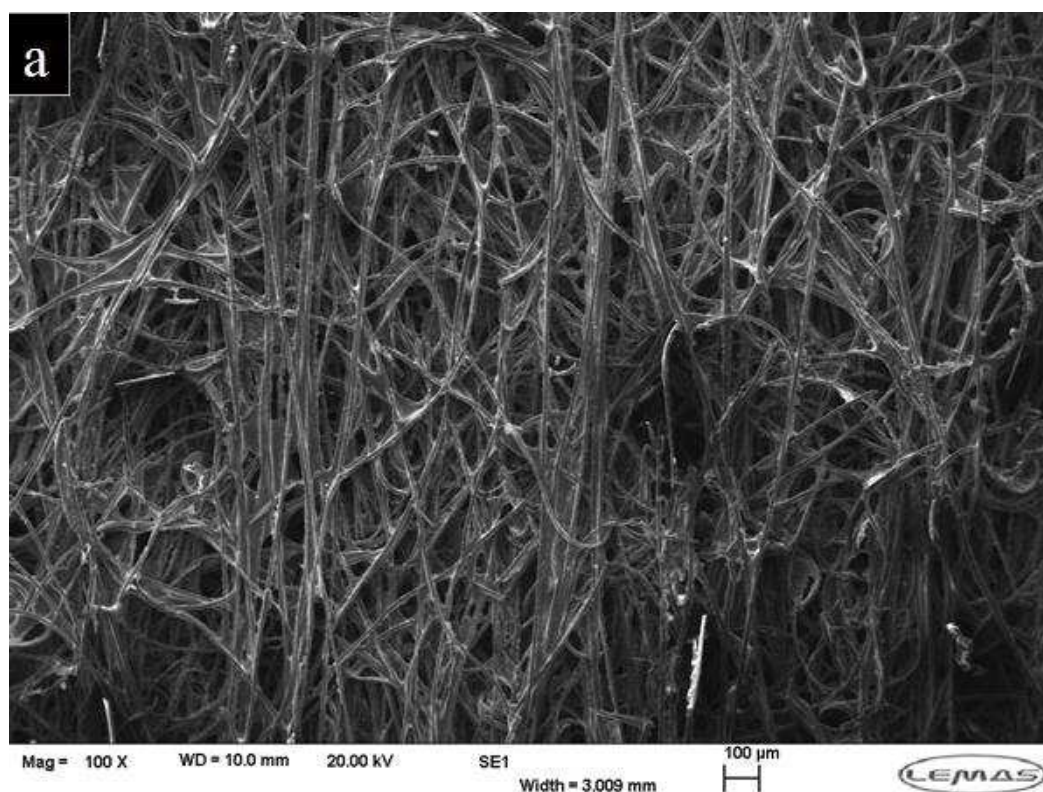
Fig. 2: Measured pressure gradient as a function of the gas velocity for an SGL 10BA sample. The solid line represents the curve-fitting line.

3.2 Through-plane gas permeability of MPL-coated GDLs

Figure 3 shows typical SEM images for the surface of the carbon substrate before and after the MPL coating and Figure 4 shows the experimental data of the pressure gradient as a function of the nitrogen velocity for the SGL 10BA carbon substrate coated with various carbon loadings. It is evident from Figure 4 that, for a given velocity and regardless of the carbon black used, the pressure gradient increases as the carbon loading increases in the MPL. This is clearly due to the increase in the MPL thickness with increasing carbon loading. The calculated

permeability values for the MPL-coated GDLs prepared with both carbon blacks used are shown in Fig. 5. It should be noted that these values are the averaged permeability for six samples having the same carbon loading. As mentioned in Section 2.2, the percentage of PTFE in the MPL is fixed at a constant value, namely 20% by weight. As expected, the addition of the MPL to the base carbon substrate forms as a sandwich whose gas permeability is lower than that of the base carbon substrate by an order of magnitude.

Further, Fig. 5 shows that the permeability of the GDL coated with Vulcan is higher than that coated with Ketjenblack at lower carbon loading (i.e. $< 1.5 \text{ mg cm}^{-2}$); however, the difference in the permeability of both types decreases and becomes almost negligible as the carbon loading increases.



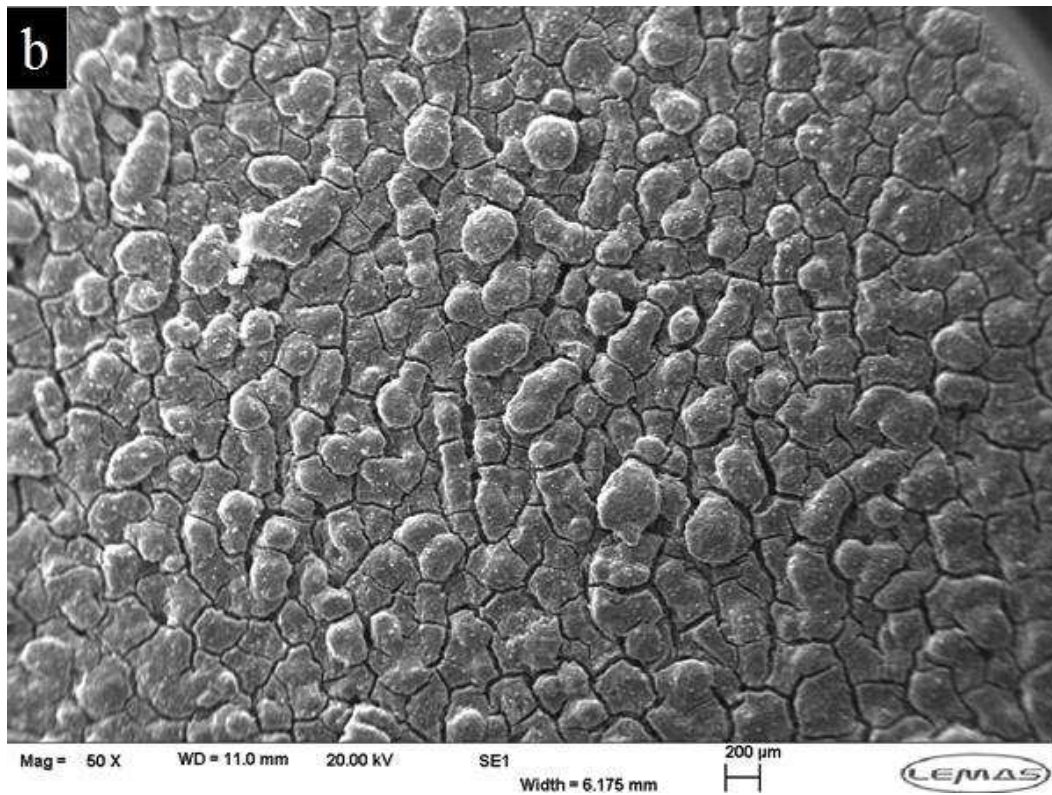


Fig. 3: Typical SEM images for the surface areas of (a) the carbon substrate, and (b) the MPL-coated sample. Carbon black used in the scanned image was Ketjenblack EC-300J.

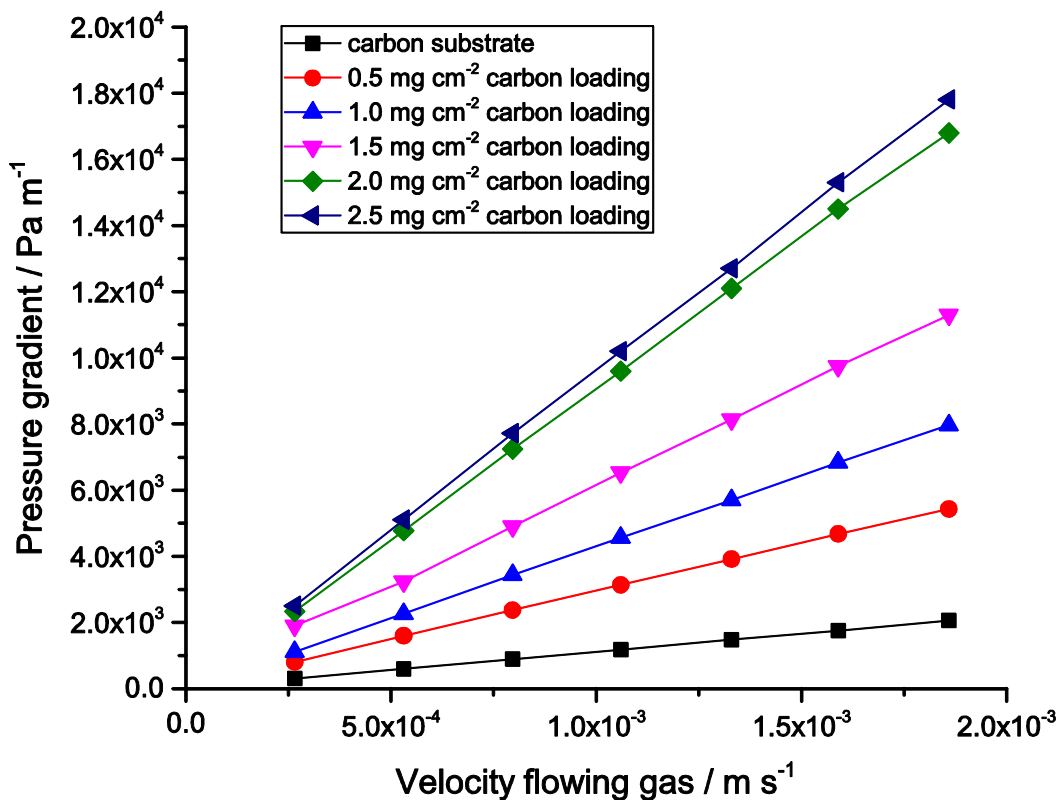
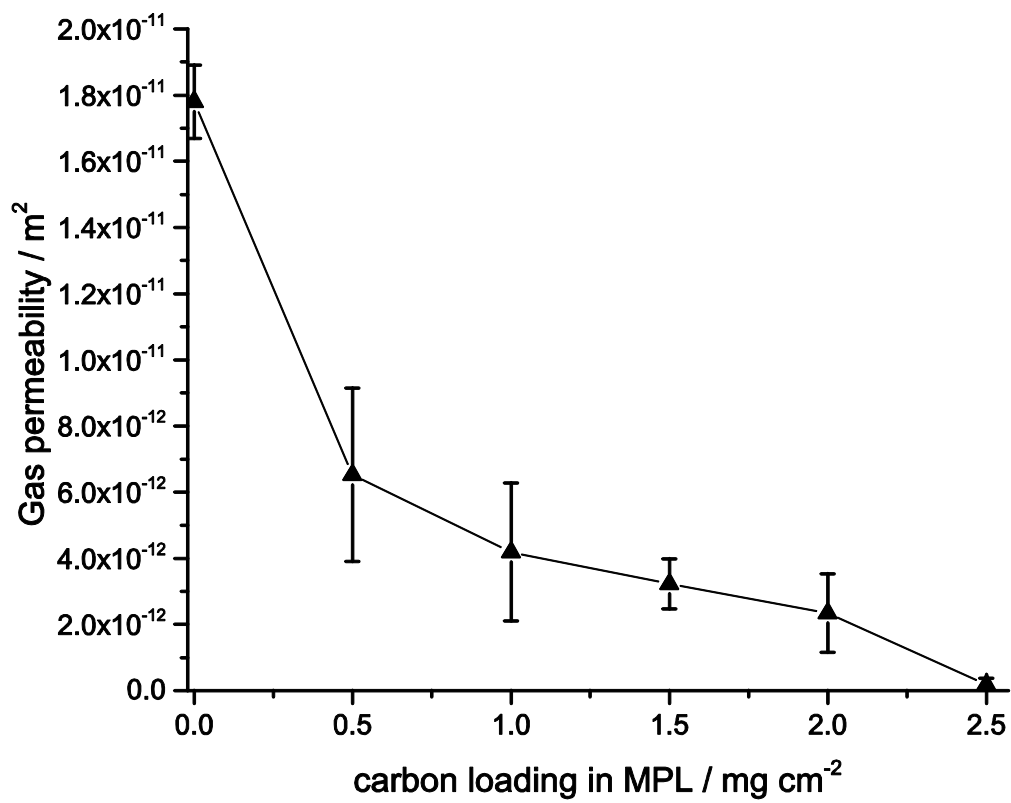
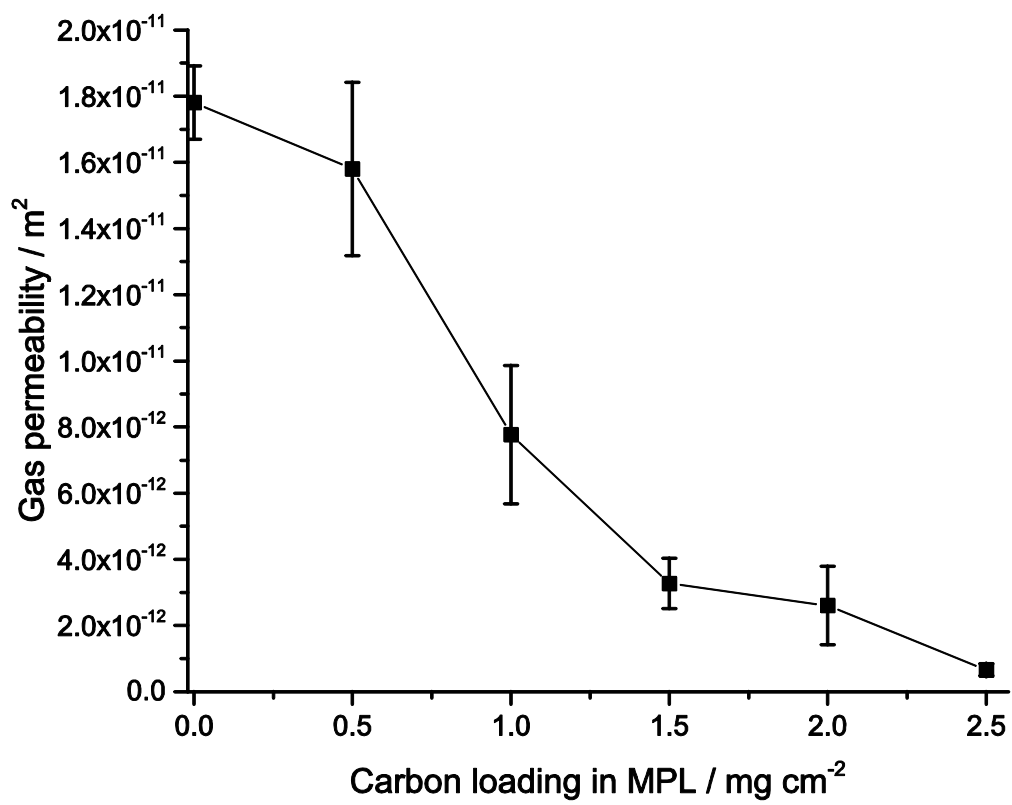


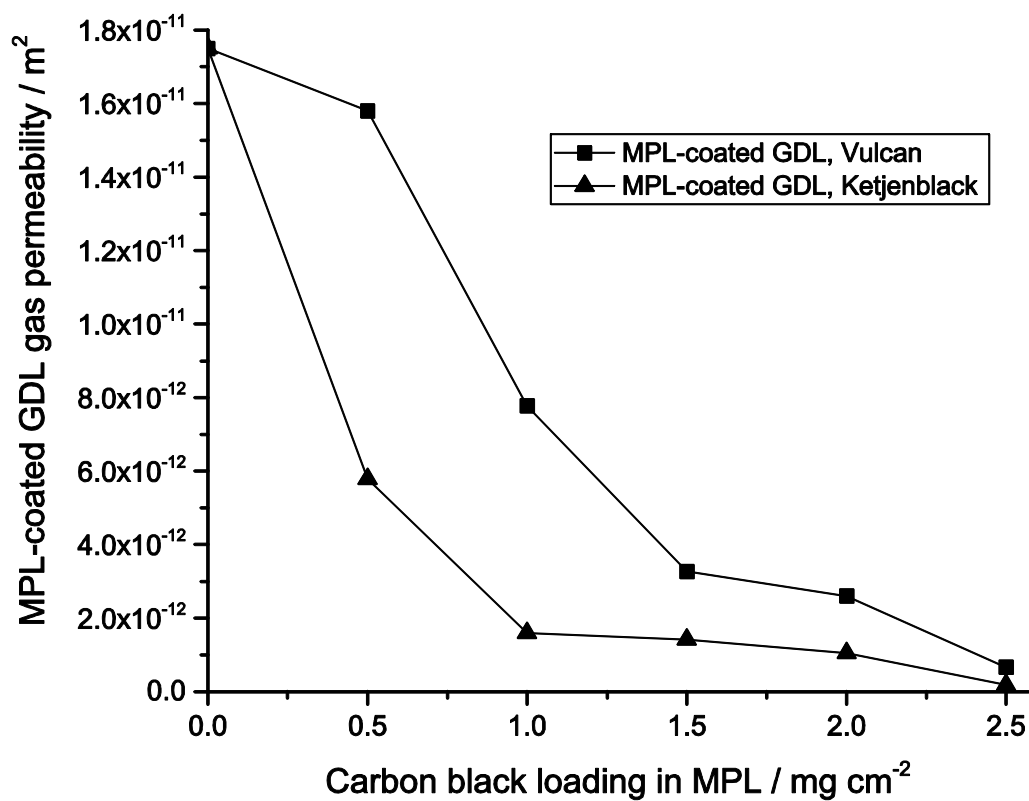
Fig. 4: Measured pressure gradient as a function of the nitrogen gas velocity for the MPL-coated carbon substrates with various carbon loadings in the MPL of 20 wt. % PTFE Ketjenblack carbon black. The samples with Vulcan XC-72R were found to have similar trends (not shown).



(a)



(b)



(c)

Fig. 5 Through-plane gas permeability of the MPL-coated GDLs as a function of carbon loading. (a) MPL-coated GDLs with Ketjenblack carbon black, (b) MPL-coated GDLs with Vulcan carbon black and (b) comparison gas permeability between both carbon black types.

3.3 Through-plane gas permeability of the MPL-coated GDL after sintering

Figure 6 shows the permeability of the MPL-coated GDLs before and after sintering. The results show that, regardless of the carbon black used in the MPL, the permeability of the coated-GDLs slightly decreases after sintering. This is most likely due to the ‘spreading effect’ that the sintering has on the MPL material, see Figure 7. In other words, sintering narrows down the cracks existing in the MPL (due to the above-mentioned spreading effect) and eventually increases the gas (mass) resistance. In addition, the pore size distribution of the samples before and after sintering affected by the fraction of micropores, mesopores and macropores of the carbon blacks. In literature it was found that Ketjenblack possess a significant fraction of micropores (25 % of the total pore volume) in contrast to Vulcan with only 15 % of the total pore volume [46]. Also, the total pore volume presented in Table 2 reveals that the Ketjenblack to be filled with ionomer and to leads to a decrease in gas permeability. The MPL coating of the GDL leads to a reduction of the average pore diameter with increasing and to small decrease in total pore volume by indicating that part of the MPL becomes enriched into the carbon-fibre substrate [26].

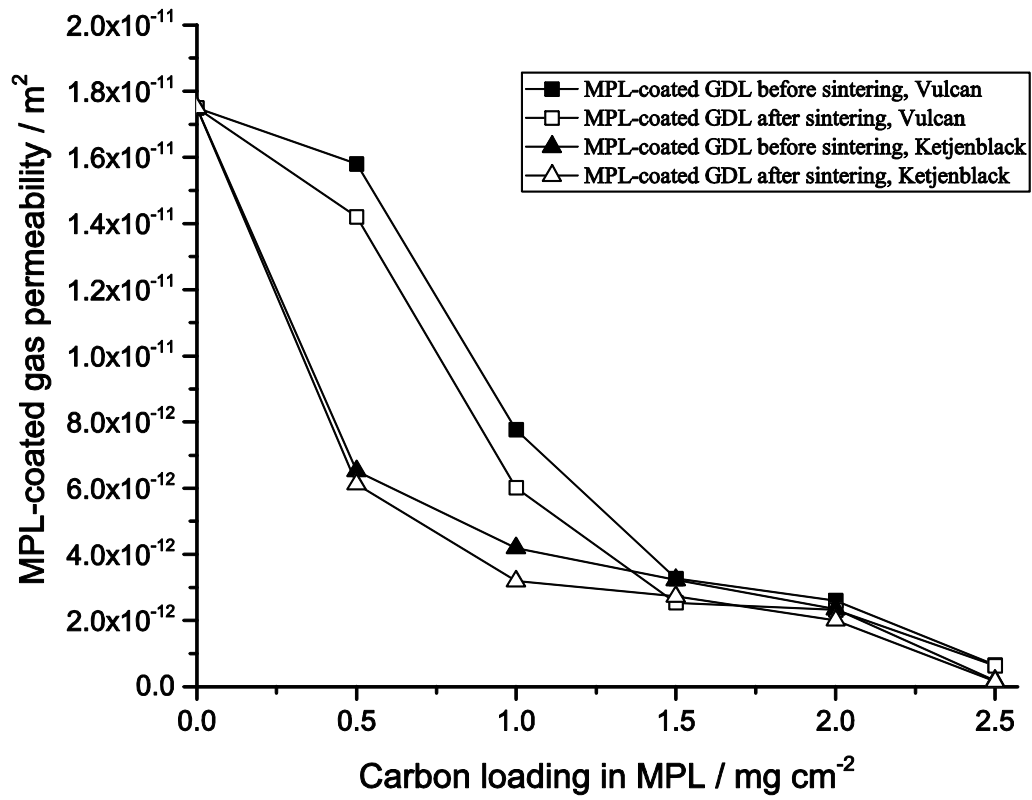


Figure 6: Through-plane gas permeability of the MPL-coated GDLs before and after sintering the MPL-coated GDLs.

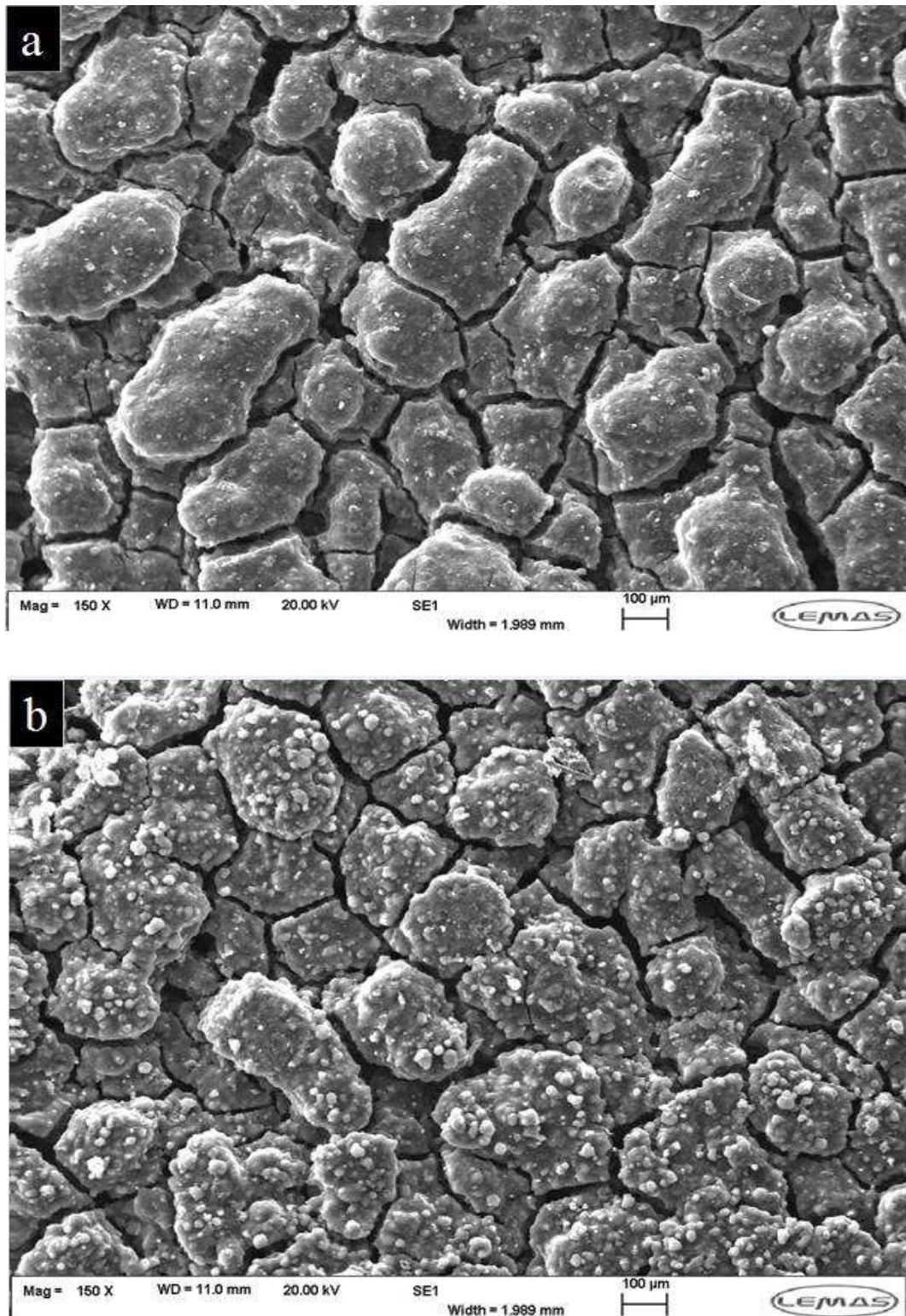


Figure 7. SEM images for the MPL with 1.5 mg cm^{-2} Ketjenblack carbon loading (a) before sintering, and (b) after sintering.

3.4 Through-plane gas permeability of MPLs

Equation (5) was used to estimate the through-plane gas permeability of the MPLs of the coated samples. All the parameters required to estimate the permeability of the MPL were determined as explained in Sections 2.1, 3.1 and 3.2. These parameters are the gas permeability and the thickness values of both the carbon substrate and the MPL-coated GDL and also the thickness of the MPL, see Fig. 5 and Fig. 9. In accordance with the procedures adopted in the literature [25, 33, 36], the MPL thickness has been estimated in this work through the use of cross-sectional SEM images of the coated GDLs, see Fig. 8. In order to minimise the distortion of the through-plane structure of the coated MPL-coated GDLs, they were cooled with liquid nitrogen before breaking the samples. Fig. 8 shows a typical cross-sectional SEM image of the MPL-coated GDL sample. It is clear from the figure that the thickness of the coated MPL is widely variable. Therefore, in order to have a relatively representative value for the MPL thickness, the latter was visually estimated at as many locations as possible in order to obtain the average value that was employed in the calculations.

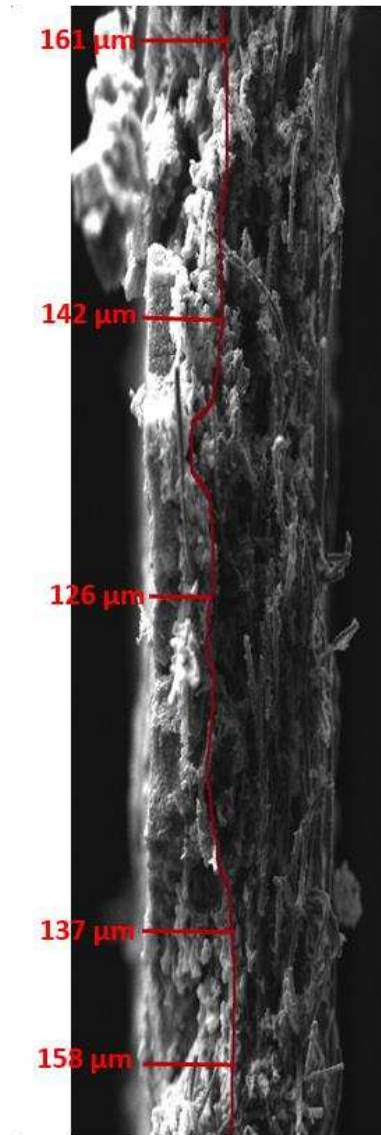
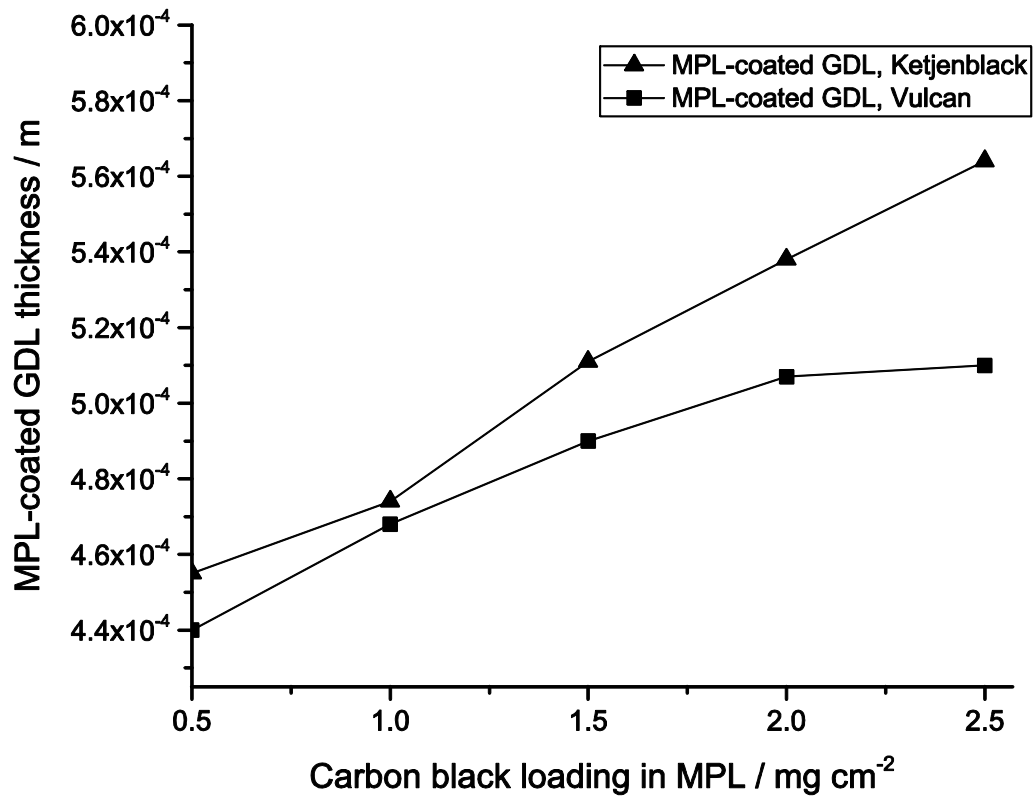
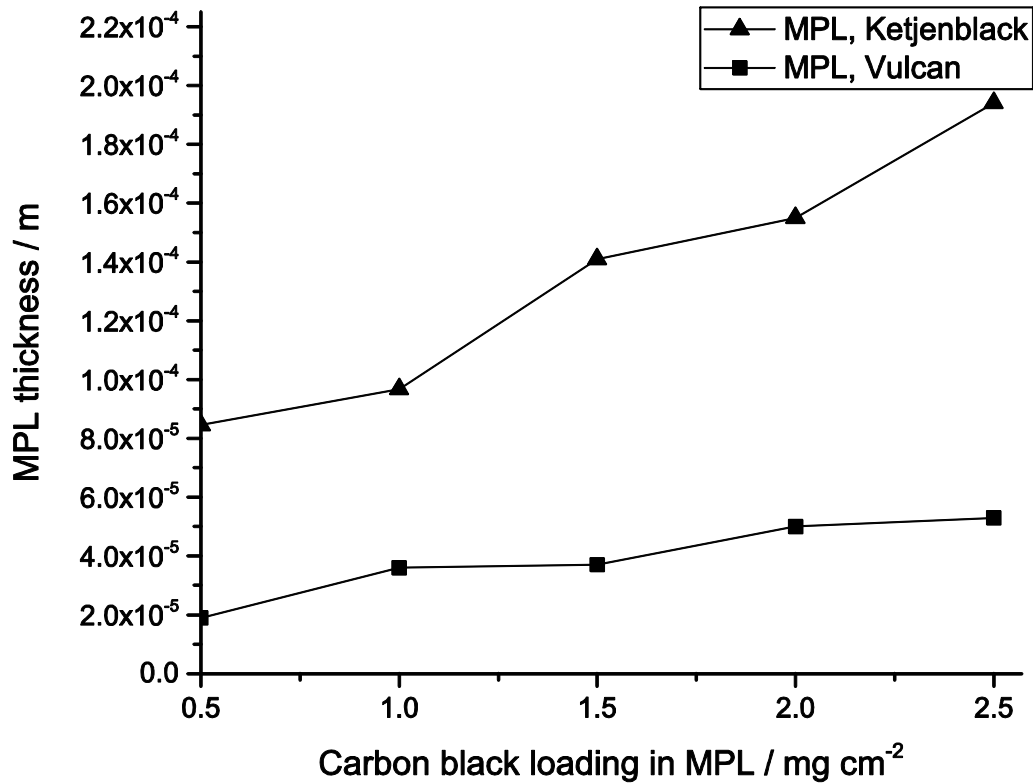


Figure 8. A typical cross-sectional SEM image for an MPL-coated GDL with a carbon loading of 2 mg cm^{-2} .



(a)



(b)

Figure 9. The thickness of (a) the MPL-coated GDL and (b) the MPL as a function of carbon loading.

Fig. 10 shows the permeability values calculated for the MPLs with different carbon loadings. It shows that the permeability decreases with increasing carbon loading. However, this should not be the case. Regardless of the carbon loading, the permeability values for the MPLs should be ideally the same for all the coated samples. This is because of the fact that the composition is the same for all the MPLs: 80% carbon black and 20 wt. % PTFE. In other words, the MPL material does not change as the carbon loading changes and therefore its permeability should be ideally the same as the latter is an intrinsic property of the material. This signifies that the

current approach of estimating the MPL permeability, by either using the micrometre or the cross-section SEM images of the MPL-coated GDLs, appears to lead to rather inaccurate results. This is most likely due to the significant penetration of the MPL material into the body of the carbon substrates which sheds more light on the uncertainty in the estimation of the MPL thickness [21]. The accurate estimation of the permeability of the MPL may be a topic of a future work.

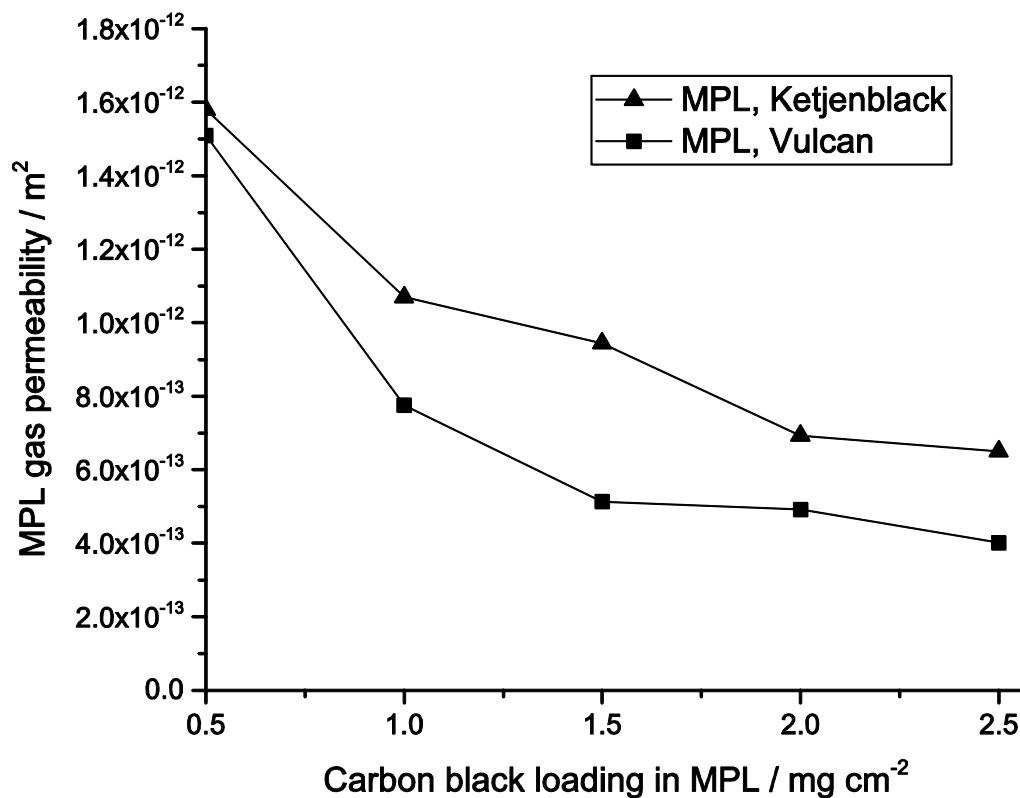


Figure 10. The gas permeability of the MPL as a function of carbon loading.

4. Conclusions

The gas permeability of the GDLs coated with MPLs having various carbon loadings has been experimentally estimated using two types of commonly-used carbon blacks: Ketjenblack and Vulcan XC-72R, the permeability of the MPL was estimated through the employment of (i) the measured permeability and thickness of the GDL before and after the MPL-coating, and (ii) the cross-section SEM images of the coated GDLs to estimate the thicknesses of the MPLs. The following are the main conclusions: the MPL-coating reduces the permeability of the GDL by at least one order of magnitude and this is clearly due to the significantly lower permeability of the MPLs. The permeability of the MPL was found to change significantly with the carbon loading, despite the use of the invariable weight composition for all the MPLs coated, namely 20% PTFE and 80% carbon black. This is mainly due to the inaccurate estimation of the MPL thickness using either the micrometre or the cross-sectional images SEM of the coated GDL which do not account for the penetrating part of the MPL. The MPL sintering was found to slightly decrease the permeability of the GDL as it appears to narrow the gaps between the cracks in the MPL. Finally, it should be noted that all of the above findings are applicable to both the carbon blacks investigated.

Acknowledgments

The first author gratefully acknowledges the Management of Federal College of Education, Obudu and the Nigeria Government for their financial support. The authors would like to thank SGL Technologies GmbH, Germany for providing the GDL sample material. Also, the Cabot Corporation, USA for providing Vulcan XC72R used as corresponding carbon black for this

work. The technical supports of Paul Crosby and Gurdev Bhogal for the experimental work carried out in this study are gratefully acknowledged.

Nomenclature

D Circular diameter / m

K Permeability / m^2

L Thickness of porous medium / m

Q Volumetric flow rate / L min^{-1}

v Velocity / m s^{-1}

Greek symbols

μ Fluid viscosity / Pa s

ρ Density / kg m^{-3}

References

- [1] D. Feroldi, M. Basualdo, PEM fuel cells with bio-ethanol processor systems, *Green Energy and Technology* 87 (2012) 49-72.
- [2] Z. Xie, G. Chen, X. Yu, M. Hou, Z. Shao, S. Hong, C. Mu, Carbon nanotubes grown in situ on carbon paper as a microporous layer for proton exchange membrane fuel cells, *Int. J. Hydrogen Energy* 40 (2015) 8958-8965
- [3] G. Hu, G. Li, Y. Zheng, Z. Zhang, Y. Xu, Optimization and parametric analysis of PEMFC based on an agglomerate model for catalyst layer, *J. the Energy Institute* 87 (2014) 163 – 174.
- [4] E. Afshari, M. Ziaei-Rad, M. M. Dehkordi, Numerical investigation on a novel zigzag-shaped flow channel design for cooling plates of PEM fuel cells, *J. the Energy Institute* (2016) 1-12.
- [5] H. Zamora, P. Cañizares, M. A. Rodrigo, Improving of microporous layer based on advanced carbon materials for high temperature proton exchange membrane fuel cell electrodes, *Fuel Cells* 2 (2015) 391-397.
- [6] F. Zabihian, A. S. Fung, Performance analysis of hybrid solid oxide fuel cell and gas turbine cycle (part II): Effects of fuel composition on specific work and efficiency, *J. the Energy Inst.* 87 (2014) 28 – 34.
- [7] S. Subramanian, G. Rajaram, K. Palaniswamy, V. R. Jothi, Comparison of perforated and serpentine flow fields on the performance of proton exchange membrane fuel cell, *J. the Energy Institute* (2016) 1-9.

- [8] S. Subramanian, G. Rajaram, K. Palaniswamy, V. R. Jothi, Comparison of perforated and serpentine flow fields on the performance of proton exchange membrane fuel cell, *J. Energy Institute* (2016) 1-9.
- [9] M. S. Ismail, A. Hassanpour, D. B. Ingham, L. Ma, M. Pourkashanian, On the compressibility of gas diffusion layers in proton exchange membrane fuel cells, *Fuel Cells* 3 (2012) 375-383.
- [10] F. Zabihian, A. S. Fung, Performance analysis of hybrid solid oxide fuel cell and gas turbine cycle (part I): Effects of fuel composition on output power, *J. Energy Institute* 87 (2014) 18 – 27.
- [11] M. Mathias, J. Roath, J. Fleming, W. Lehnert, Diffusion media materials and characterisation, *Handbook of Fuel Cells* 3 (2010) 517-537.
- [12] P. M. Wilde, M. Mandle, M. Murata, N. Berg, Structural and physical properties of GDL and GDL/BPP combinations and their influence on PEMFC performance, *Fuel Cells* 4 (2004) 180-184.
- [13] S. Xue, G. Yin, Methanol permeability in sulfonated poly(etheretherketone) membranes: A comparison with Nafion membranes, *European Polymer Journal* 42 (2006) 776-785.
- [14] S. B. Park, S. Kim, Y. i. Park, M. H. Oh, Fabrication of GDL microporous layer using PVDF for PEMFCs, *J. Physics* 165 (2009) 012046-012051.
- [15] G. Valayutham, J. Kaushik, N. Rajalakshmi, K. S. Dhathathreyan, Effect of PTFE content in gas diffusion media and microlayer on the performance of PEMFC tested under ambient pressure, *Fuel Cells* 7 (2007) 314-318.

- [16] R. P. Ramasamy, E. C. Kumbur, M. M. Mench, W. Liu, D. Moore, M. Murthy, Investigation of micro – and micro-porous layer interaction in polymer electrolyte fuel cells, *Int. J. Hydrogen Energy* 33 (2008) 3351-3367.
- [16] N. Parikh, J. S. Allen, R. S. Yassar, Microstructure of gas diffusion layers for PEM fuel cells, *Fuel Cell* 12 (2012) 382-390.
- [18] F. Barbir, *PEM fuel cells; Theory and Practice*. Academic Press, UK (2013) 73.
- [19] M. Hossain, S. Z. Islam, P. Pollard, Investigation of species transport in a gas diffusion layer of a polymer electrolyte membrane fuel cell through two-phase modelling, *Renewable Energy* 51 (2013) 404-418
- [20] S. Park, J. W. Lee, B. N Popov, A review of gas diffusion layer in PEM fuel cells: Materials and designs *Int. J. Hydrogen Energy* 37 (2012) 5850-5865.
- [21] T. Kitahara, T. Konomi, H. Nakajima, Microporous layer coated gas diffusion layers for enhanced performance of polymer electrolyte fuel cells *J. Power Sources* 195 (2010) 2202-2210.
- [22] L. R. Jordan, A. K. Shukla, T. Behrsing, N. R. Avery, B. C. Muddle, M. Forsyth, Diffusion layer parameters influencing optimal fuel cell performance, *J. Power Sources* 86 (2000) 250-254.
- [23] M. Mortazavi, K. Tajir, Effect of the PTFE content in the gas diffusion layer on water transport in polymer electrolyte fuel cells (PEFCs), *J. Power Sources* 245 (2014) 236-244.

- [24] J. Itonen, M. Mikkola, G. Linbergh, Flooding of gas diffusion backing in PEFCs: Physical and Electrochemical Characterisation, *J. Electrochemical Society* 151 (2004) A1152-A1161.
- [25] M. S. Ismail, D. Borman, T. Damjanovic, D. B. Ingham, M. Pourkashanian, On the through-plane permeability of microporous layer-coated gas diffusion layers used in proton exchange membrane fuel cells, *Int. J. Hydrogen Energy* 36 (2011) 10392-10402.
- [26] S. Park, J. W. Lee, B. N. Popov, Effect of carbon loading in microporous layer on PEM fuel cell performance, *J. Power Sources* 163 (2006) 357-363.
- [27] M. S. Ismail, T. Damjanovic, D. B. Ingham, M. Pourkashanian, A. Westwood, Effect of polytetrafluoroethylene-treatment and microporous layer-coating on the electrical conductivity of gas diffusion layers used in proton exchange membrane fuel cells, *J. Power Sources* 195 (2010) 2700-2708.
- [28] H. M. Chang, M. H. Chang, Effect of gas diffusion layer with double-side microporous layer coating on polymer electrolyte membrane fuel cell performance, *J. Fuel Cell Science and Technology* 10 (2013) 021005-10.
- [29] T. H. Ko, W. S. Kuo, S. H. Su, J. H. Lin, W. H. Chen, Effect of multi micro porous layer in proton exchange membrane fuel cell, *Exchange Membrane Fuel Cell* (2010) 1-4.
- [30] C. Chan, N. Zamel, X. Li, J. Shen, Experimental measurement of effective diffusion coefficient of gas diffusion layer/microporous layer in PEM fuel cells, *Electrochimica Acta* 65 (2012) 13-21.

- [31] A. Z. Weber, J. Newman, Effects of microporous layers in polymer electrolyte fuel cells, *J. Electrochemical Society* 152 (2005) A677-A688.
- [32] M. S. Ismail, T. Damjanovic, D. B. Ingham, L. Ma, M. Pourkashanian, Effect of polytetrafluoroethylene-treatment and microporous layer-coating on the in-plane permeability of gas diffusion layers used in proton exchange membrane fuel cells *J. Power Sources* 195 (2010) 6619-6628.
- [33] Q. Ye, T. V. Nguyen, Three-Dimensional Simulation of Liquid Water Distribution in a PEMFC with Experimentally Measured Capillary Functions, *J. Electrochemical Society* 154 (2007) B1242-B1251.
- [34] J. T. Gostick, M. W. Fowler, M. D. Pritzker, M. A. Ioannidis, L. M. Behra, In-plane and through-plane gas permeability of carbon fibre electrode backing layers, *J. Power Sources* 162 (2006) 228-238.
- [35] X. Wang, T. V. Nguyen, D. S. Hussey, D. L. Jacobson, An experimental study of relative permeability of porous media used in porous exchange membrane fuel cells, *J. Electrochemical Society* 157 (2010) B1777-B1782.
- [36] D. Shou, Y. Tang, L. Ye, J. Fan, F. Ding, Effective permeability of gas diffusion layer in proton exchange membrane fuel cells, *Int. J. Hydrogen Energy* (2013) 3810519-10526.
- [37] V. Gurau, M. J. Bluemle, E. S. De Castro, Y. M. Tsou, T. A. Zawodzinski Jr., J. A. Mann Jr., Characterization of transport properties in gas diffusion layers for proton exchange membrane fuel cells 2: Absolute permeability, *J. Power Sources* 160 (2007) 1156-1162.

- [38] J. G. Pharoah, On the permeability of gas diffusion media used in PEM fuel cells, *J. Power Sources* 144 (2005) 77-82.
- [39] M. S. Ismail, T. Damjanovic, K. Hughes, D. B. Ingham, L. Ma, M. Pourkashanian, M. Rosli, Through-plane permeability for untreated and PTFE-treated gas diffusion layers in proton exchange membrane fuel cells, *J. Fuel Cell Science and Technology* 7 (2010) 1-7.
- [40] A. Tamayol, F. McGregor, M. Bahrami, Single phase through-plane permeability of carbon paper gas diffusion layers, *J. Power Sources* 204 (2012) 94-99.
- [41] M. I. Ismail, K. J. Hughes, D. B. Ingham, L. Ma, M. Pourkashanian, Effects of anisotropic permeability and electrical conductivity of gas diffusion layers on the performance of proton exchange membrane fuel cells, *Applied Energy* 95 (2012) 50-63.
- [42] X. L. Wang, H. M. Zhan, J. L. Zhang, H. F. X, Z. Q. Tian, J. Chen, H. X. Zhong, Y. M. Liang, B. L. Yi, Micro-porous layer with composite carbon black for PEM fuel cells *Electromica Acta* 51 (2006) 4909-4915.
- [43] V. Gurau, M. J. Bluemle, E. S. De Castro, Y. M. Tsou, T. A. Zawodzinski Jr., J. A. Mann Jr., Characterization of transport properties in gas diffusion layers for proton exchange membrane fuel cells 1: Wettability (internal contact angle to water and surface energy of GDL fibres, *J. Power of Sources* 160 (2006) 1156-1162.
- [44] M. V. Williams, E. Begg, L. Bonville, H. R. Kunz, J. M. Fenton, Characterisation of gas diffusion layers for PEMFC, *J. Electrochemical Society* 151 (2004) A1173-A1180.
- [45] O. M. Orogbemi, D. B. Ingham, M. S. Ismail, K. J. Hughes, L. Ma, M. Pourkashanian, The effects of the composition of microporous layers on the permeability of gas diffusion

layers used in polymer electrolyte fuel cells. *Int. J. Hydrogen Energy* (2016) 1-7.

DOI:10.1016/j.ijhydene.2016.09.160.

- [46] J. Yu, M. N. Islam, T. Matsuura, M. Tamano, Y. Hayashi, M. Hori, Improving the performance of a PEMFC with Ketjenblack EC-600JD carbon black as the material of the microporous layer. *Electrochemical and Solid-State Letters* 8 (2005) A320-A323.